2018

Land-Cover Change and the "Dust Bowl" Drought in the U.S. Great Plains

Qi Hu

Jose Abraham Torres-Alavez

Matthew S. Van Den Broeke

Land-Cover Change and the "Dust Bowl" Drought in the U.S. Great Plains

QI HU

School of Natural Resources, and Department of Earth and Atmospheric Sciences, University of Nebraska–Lincoln, Lincoln, Nebraska

JOSE ABRAHAM TORRES-ALAVEZ AND MATTHEW S. VAN DEN BROEKE

Department of Earth and Atmospheric Sciences, University of Nebraska–Lincoln, Lincoln, Nebraska

(Manuscript received 3 August 2017, in final form 15 February 2018)

ABSTRACT

The North American Dust Bowl drought during the 1930s had devastating environmental and societal impacts. Comprehending the causes of the drought has been an ongoing effort in order to better predict similar droughts and mitigate their impacts. Among the potential causes of the drought are sea surface temperature (SST) anomalies in the tropical Pacific Ocean and strengthened local sinking motion as a feedback to degradation of the land surface condition leading up to and during the drought. Limitations on these causes are the lack of a strong tropical SST anomaly during the drought and lack of local anomaly in moisture supply to undercut the precipitation in the U.S. Great Plains. This study uses high-resolution modeling experiments and quantifies an effect of the particular Great Plains land cover in the 1930s that weakens the southerly moisture flux to the region. This effect lowers the average precipitation, making the Great Plains more susceptible to drought. When drought occurs, the land-cover effect enhances its intensity and prolongs its duration. Results also show that this land-cover effect is comparable in magnitude to the effect of the 1930s large-scale circulation anomaly. Finally, analysis of the relationship of these two effects suggests that while lowering the precipitation must have contributed to the Dust Bowl drought via the 1930s land-cover effect, the initiation of and recovery from that drought would likely result from large-scale circulation changes, either of chaotic origin or resulting from combinations of weak SST anomalies and other forcing.

1. Introduction

Severe drought during the warm seasons from 1932 to 1938 in the U.S. Great Plains was coined the "Dust Bowl" to describe the frequent and massive dust storms during the drought. Because of its destructive impacts on individual lives and society, causes of the drought have been sought intensely for the purposes of prediction and mitigation.

The Dust Bowl drought has been considered "highly unusual" (Cook et al. 2009) because such a severe drought persisted in a decade when there were "surprisingly weak" sea surface temperature (SST) anomalies in the tropical Pacific Ocean (Schubert et al. 2004). Strong SST anomalies in the tropical Pacific (e.g., during El Niño/La Niña events) influence precipitation variations in North America and other regions around the globe (e.g., Ropelewski and Halpert 1986; Hu and Feng 2001). Extended strong SST anomalies likely contribute to lasting anomalies in precipitation. During the 1930s, the El Niño/La Niña in the tropical Pacific Ocean went through two cycles, with weak to moderate El Niño events in 1930–33 and again in 1935–37 and a weak La Niña event following each of them (Wolter and Timlin 2011). In the North Atlantic Ocean, where the warm SST anomaly associated with the Atlantic multidecadal oscillation (AMO; Enfield et al. 2001) favors less warm season precipitation in the central United States, the SST anomalies were in a transition from a cold to a warm phase during 1920–40 (e.g., Hu and Feng 2008). Although the warming SST in the North Atlantic Ocean in the 1930s favored less warm season precipitation in the U.S. Great Plains, that effect would be insufficient to result in a drought of Dust Bowl scale because the remote effect of the SST anomalies is weak and often inconsistent during the AMO warm phase (Hu and Feng

Corresponding author: Dr. Qi Hu, qihu@unl.edu

DOI: 10.1175/JCLI-D-17-0515.1

2008; Hu et al. 2011; Hu and Veres 2016). When also considering that ENSO strongly influences interannual variation of precipitation in addition to the decadal-scale AMO effect in midlatitude North America (Hu and Feng 2012), we would have expected to have two weak warm season droughts in the Great Plains during the 1930s. This expectation based on the SST effects is supported by results from both modeling (Hoerling et al. 2009; Schubert et al. 2004; Seager et al. 2005; Cook et al. 2009) and statistical analysis of SST and warm season precipitation anomalies in the U.S. Great Plains (e.g., Hu and Feng 2008).

Hoerling et al. (2009, p. 1) examined ensembles from each of three different atmospheric general circulation models (AGCMs) that were integrated from 1903–2004 with observed monthly global SST, and suggested that ''that region's [U.S. Great Plains] drought exhibited little sensitivity to SST conditions during the Dust Bowl period.'' Schubert et al. (2004) showed that local and regional land–atmosphere interactions in their AGCM experiments played a major role in the Dust Bowl drought after weak SST anomalies in the tropical Pacific initiated the drought. The land–atmosphere interaction was further investigated in an AGCM study by Cook et al. (2009). They examined the human land degradation and subsequent changes in surface albedo and atmospheric dust/aerosol loading. Their results showed that in the given global SST anomalies in the 1930s the dust loading after crop failures from initial dry conditions could have reduced net surface radiation as a result of increased surface albedo, so that additional subsidence occurred to suppress precipitation and enhance the drought, similar to that described by Charney (1975).

While this land–atmosphere interaction process and its induced subsidence could enhance the drought in one failed cropping season, how it may repeat itself over several years remains a question, especially in the Great Plains where the warm season circulation is characterized by the Great Plains southerly low-level jet (GPLLJ) (Bonner and Paegle 1970; Mo et al. 1997; Higgins et al. 1998). The GPLLJ transports large amount of moisture from the Gulf of Mexico to the Great Plains. Along the boundary between the moist air and subsidence and dry areas to its north and west forms dryline and mesoscale convective systems that can bring intense convection and precipitation (Hane et al. 1997) to weaken or reverse the drought. Thus, some processes in addition to the local subsidence must act to undercut the moisture supply. Those processes have to repeat year after year in order to sustain and intensify the multiyear Dust Bowl drought.

In this work, we show a mechanism that could have sustained the multiyear drought in the 1930s, as well as droughts of similar magnitude in the Great Plains should the same condition recur. In this mechanism, land-cover change in the Great Plains plays an important role. This change evolved from presettlement (1850) to the 1930s when the U.S. Great Plains experienced substantial agricultural growth (e.g., Cunfer 2005). A cost of this growth and expansion was the loss of native vegetation; about 43% of native grasslands in the region were converted into dryland croplands and pastures during that period (Table 1). A direct consequence of these changes was reduced soil water storage, because of loss of connection to deep soil water by deep rooting systems of the native vegetation and enhanced surface evapotranspiration in crops. These changes altered the surface albedo and the surface and atmospheric energy and water budgets, causing sinking motion (e.g., Cook et al. 2009). Although these changes may intensify a drought, their effects are local and passive because they will affect primarily the local recycling of moisture. This recycling contributes to less than 20% of Great Plains precipitation (Brubaker et al. 1993). More than 80% of the moisture making up the region's precipitation is transported into the region by the regional atmospheric circulation, including the GPLLJ. When this transport is weakened or interrupted, the supply of the other 80% of moisture is suppressed, and severe drought may occur and persist. We will show that an additional (and indirect) effect of the land-cover change in the Great Plains from presettlement to the 1930s is to set up a regional condition that weakened the GPLLJ and the moisture supply to the Great Plains. In the absence of strong remote SST forcing (e.g., Cook et al. 2009; Hoerling et al. 2009), this effect of land-cover change creates conditions favorable for development of the prolonged 1930s Dust Bowl drought.

2. Data and methods

To quantify this effect, we use the Weather Research and Forecasting Model version 3.6 (WRF3.6; Skamarock et al. 2008) coupled with the NCAR Community Land Model version 4.0 (CLM4.0; Oleson et al. 2010; Lawrence et al. 2011). The CLM4.0 is used in this study because recent results indicate consistent performance of CLM4.0 in the U.S. Great Plains (Van Den Broeke et al. 2017). The CLM4.0 consists of five subgrid surface land-cover types including lakes, wetland, and vegetation, with vegetation being further divided into seven plant functional types. Each type is specified with a representative leaf and stem area index and canopy height. For a given surface land-cover type the surface albedo is calculated using a two-stream approximation of radiative transfer in the atmosphere (Oleson et al.

TABLE 1. Percentage of area covered by different land-cover classifications in the three periods in the U.S. Great Plains, from 30°–43°N and 95°–105°W (inside the red box in Fig. 1b). Boldface type highlights land cover conditions during the Dust Bowl drought.

Land-cover classification	Presettlement (1850)	Dust Bowl (1935–38)	Present day (2011)
Dryland cropland and pasture	0	**31**	4
Grassland	70	**41**	38
Mixed dryland/irrigated cropland	0	**0**	24
Deciduous and broadleaf forest	4	**4**	4
Savanna	10	**2.5**	0
Urban	0	**0**	5
Barren or sparsely vegetated land	3	**10**	0.5
Other (water bodies, shrubland, and evergreen needle leaf forest)	13	**11.5**	24.5

2010), as detailed in the literature (e.g., Sellers 1985; Oleson et al. 2010). Additional details of CLM4.0 and its coupling with WRF3.6 are presented by Van Den Broeke et al. (2017).

In the recent decade, WRF and its land surface modules have been tested and improved, and have become a primary tool for studying dynamic processes in weather and climate. A key feature of the WRF is its high spatial resolution, allowing us to couple it with high-resolution land surface modules (e.g., CLM4.0) and land-cover data to more accurately describe spatial variations in land cover and land–atmosphere interactions. As indicated by Seager et al. (2005), the coarse resolution in GCMs (on the order of 100 km) limits details in land surface information and processes. It can cause the models to overestimate the influence of SST anomalies and the effect of the internal variability of the atmosphere on droughts, and to underestimate the effects of land surface processes. Such biases can be overcome by high-resolution regional models.

The WRF Model used in this study has two nested domains. The outer domain has a horizontal resolution of 12 km, covering North America and parts of adjacent oceans (approximately 140°–60°W and 23°–51°N). The inner domain has a 4-km horizontal resolution, covering the U.S. Great Plains (approximately 85°–110°W and 29.8°–43.6°N, the area in Fig. 1a). The model has 29 hybrid sigma-pressure levels in the vertical direction with the highest level fixed at 100 hPa. Among physical parameterizations, the WRF used the Kain–Fritsch scheme to describe convection (Kain and Fritsch 1990), the single-moment five-class scheme for cloud microphysics (Hong et al. 2004), the Yonsei University (YSU) scheme for the planetary boundary layer (Hong et al. 2006), and Dudhia (1989) and the Rapid Radiative Transfer Model (RRTM; Mlawer et al. 1997) for shortwave and longwave radiation transfer. These methods have been evaluated extensively and shown to be relevant for use in midlatitude North America (Hong et al. 2006; Bukovsky and Karoly 2009; Hu et al. 2010; Pei et al. 2014; Qiao and Liang 2015).

Initial and lateral boundary conditions for the WRF Model are provided by three different circulations: the present-day circulation and the circulations derived from the warm and the cold phase of the AMO. These circulations are used to provide different large-scale forcings (e.g., from different SST anomalies in oceanic regions) through the lateral boundary conditions to the Great Plains. The reason for using these different large-scale circulations is that, if under each of these different forcing conditions, the WRF simulation using 1930s land cover consistently produces the least amount of warm season precipitation compared to the simulations using other land covers (e.g., the presettlement and present-day land cover; discussed later in this section), the results would indicate a persistent and prominent effect of the land-cover change from the presettlement to the 1930s on the drought, regardless of different large-scale circulations and forcing conditions. We note that there are many other possible large-scale circulations that could be used to further test this persistency. In that regard, the robustness of the land-cover change effect on the drought deduced from this work remains to be further explored. We use the AMO forced circulations in addition to the observed present-day circulation in our test because the Dust Bowl drought was a decadal event (1932–38). Using the AMO-driven circulations we can examine if the Great Plains land-cover effect may deter the influence of this remote forcing, especially in the cold phase of the AMO, which favors more precipitation in the central United States, and enhance summer precipitation anomalies in the U.S. Great Plains.

In practice, the present-day circulation is derived from the North American Regional Reanalysis (NARR; 1979–present) data, which have a horizontal resolution of 33 km (Mesinger et al. 2006). Use of the present-day circulation serves two purposes in this study. One is that there was no observed circulation before 1938, and the present-day circulation offers an alternative of high

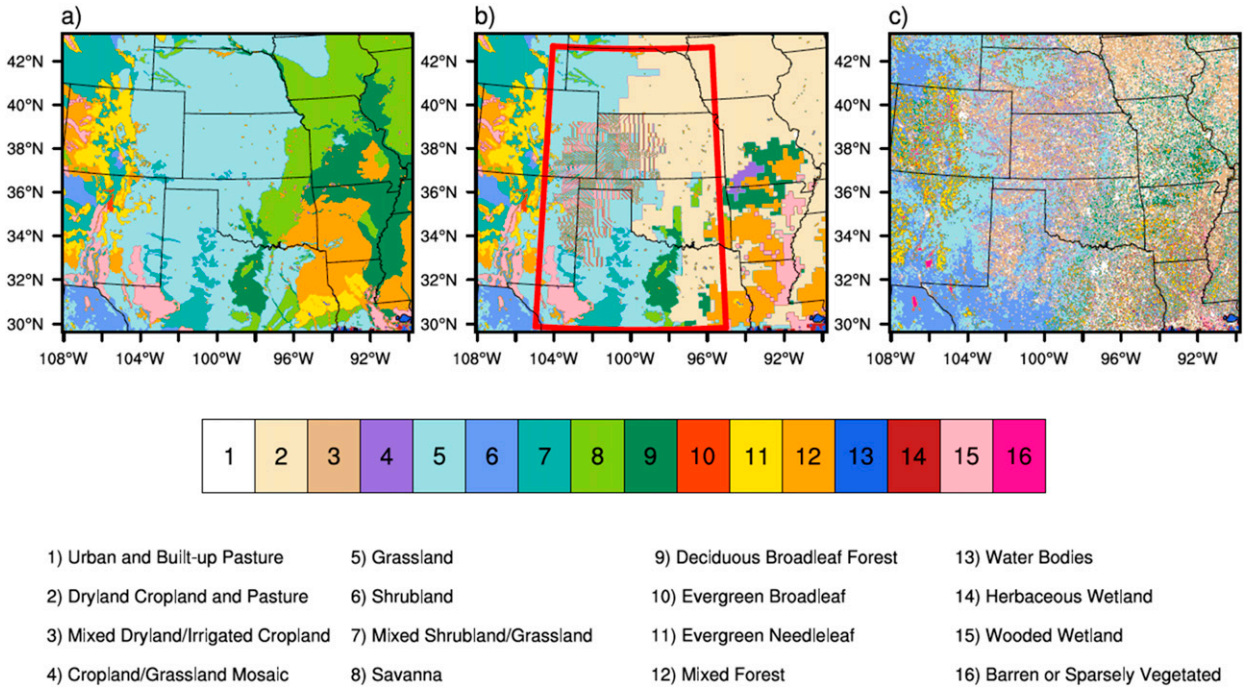

FIG. 1. Land cover in (a) presettlement, (b) the 1930s, and (c) the present day.

quality. The other is that over the present-day period from 1990 to 2002, used in this study, there were two pairs of El Niño–La Niña events in the tropical Pacific Ocean, and the SST anomalies associated with the AMO in the North Atlantic Ocean transitioned from a negative to a positive phase around 1990. The positive phase reached peak amplitude after 2002. Generally similar sequences of SST variations in both the tropical Pacific and the North Atlantic Oceans are observed from 1930 to 1942 [Wolter and Timlin 2011; also see Fig. 6a of the AMO index variation in Hu and Feng (2008)]. The similar sequence in variations of the SST anomaly in the tropical Pacific and the North Atlantic Oceans between the two periods supports the use of the atmospheric circulation in 1990–2002 to approximate that with similar interannual and decadal SST anomalies in 1930–42. Recognizing that no atmospheric circulations in two different periods are the same, we admit that this approximation merely keeps the same sequence in anomalous SST events in the tropical Pacific and the North Atlantic Ocean.

Simulations using the atmospheric circulation of 1990–2002 and the 1990 soil moisture in the initial conditions were made using the three different land covers, and the results of the last eight years were used in our analyses after removing the first five years for spinup. Because of the fixed land-cover condition in each of the simulations, we focus our analysis on the mean conditions and underlying physical processes under that specific land-cover condition. Although transient processes into and out of the integration period with fixed land cover are not examined, transient effects on precipitation variation within that period from forcings contained in the boundary conditions (e.g., El Niño, La Niña, and the AMO) are simulated.

The atmospheric circulations driven by the warm and cold phases of the AMO are obtained from prior AGCM simulations with observed AMO SST anomalies in the North Atlantic Ocean and climatological SST elsewhere (Hu et al. 2011). Those simulations generated the annual cycle of the atmospheric circulation driven by either the peak warm or cold SST anomaly during the AMO. The annual cycle of the atmospheric circulation in the AMO warm phase is used to derive the boundary conditions for the WRF. The WRF is run for five years perpetually. The same is done for the AMO cold phase. Because the perpetual runs with fixed land cover arrive at fairly stable conditions in about two years, we use the averaged results of the last three of the five years in our analysis.

In addition, in simulations with the AMO forced circulations we introduce different initial soil moisture conditions. The wet and dry soil moisture in these additional simulations was derived from the NARR data using the following procedure. We first determine the driest and the wettest May–July period in the U.S. Great

TABLE 2. Mean May–July precipitation (mm day^{-1}) averaged over the Great Plains. It is noteworthy to indicate that an initial dry soil condition does not always lead to less precipitation. The outcome is heavily affected by the large-scale circulation (e.g., the AMO) and its interaction with the land cover. That effect is secondary to the land cover, however, because the simulation with the 1930s land cover always has the least precipitation (boldfaced number in each row of this table).

	Presettlement	1930s	Present day
1995–2002 circulation	2.66	**2.53**	2.83
AMO warm phase, and initial wet soil moisture	1.98	**1.78**	1.91
AMO warm phase, and initial dry soil moisture	2.27	**2.14**	2.32
AMO cold phase, and initial wet soil moisture	2.20	**1.77**	2.52
AMO cold phase, and initial dry soil moisture	2.00	**1.68**	1.99

Plains from 1990 to 2002, and use the averaged May–July driest and wettest soil moisture values as the initial soil condition in the dry and wet simulation, respectively.

For each of these boundary conditions, the WRF is integrated to simulate Great Plains warm season precipitation with three land-cover conditions. They describe the presettlement (~1850) condition, the Dust Bowl era (1930s), and the present-day land cover (Fig. 1). These land covers are developed from sources that have a resolution at or finer than 4 km × 4 km, because our model has a 4-km resolution inner domain. Present-day land-cover data used in this study have 30-m resolution and are from the dataset developed by the Multi-Resolution Land Characteristics Consortium (MRLC), which is "a group of federal agencies who coordinate and generate consistent and relevant land cover information at the national scale for a wide variety of environmental, land management, and modeling applications." The data are accessible at http://www.mrlc.gov/nlcd11_data.php with detailed descriptions in the literature and several documents (Homer et al. 2015, and references therein).

Presettlement (1850) land cover was derived starting with the Level IV ecoregions from the U.S. Environmental Protection Agency (EPA 2013). The ecoregions represent the natural or potential vegetation that would be supported in an area (Omernik and Griffith 2014). These data were converted to the land-use and land-cover categories available in the CLM4.0. The land cover for the 1930s was derived from the U.S. Geological Survey "Reconstructed Historical Biophysical Land Cover Dataset for 1920" (Steyaert and Knox 2008) and the "Population and Environment in the U.S. Great Plains" dataset (Gutmann 2005). County-level land cover from these datasets was converted to our model land-cover categories. Land cover for the Dust Bowl period started with the 1920s land cover and was modified based on areas of known wind erosion in the Great Plains during the Dust Bowl (USDA 1954). Areas of most severe and severe wind erosion during the Dust Bowl were set to 80% and 60% bare soil, respectively. Ares of less severe wind erosion were set to have 20% bare soil cover. Other land-cover categories were preserved.

3. Results and discussion

From examining these land-cover data in the U.S. Great Plains, we find that from presettlement to the 1930s, about 43% of the native grassland and 75% of the savanna were lost to dryland croplands and pastures (cf. Figs. 1a and 1b; see Table 1). From the 1930s to the present, land cover in the Great Plains has changed to have most of the croplands irrigated at varying rates (cf. Figs. 1b and 1c).

Using these land-cover conditions we simulate Great Plains precipitation in the previously described large-scale circulations and initial soil moisture conditions. Simulated May–July total precipitation in the Great Plains is summarized in Table 2. These results show that in all three large-scale circulation scenarios with different initial soil moisture conditions (each row in Table 2), the smallest amount of precipitation always appears in the simulation that uses the 1930s land cover. Differences between simulated precipitation from using various large-scale circulations and the same land cover (each column in Table 2) show the effects of the large-scale circulation and regional soil moisture on Great Plains precipitation.

To measure the effect of the land-cover change on May–July precipitation in the Great Plains relative to the effect from large-scale circulation forcing, we take differences of the mean precipitation between simulations with different large-scale circulation and initial soil moisture condition under the same land cover (each column in Table 2). We find the difference ranging from 0.07 to 0.93 mm day^{-1}. This range is the same as the range of precipitation difference between simulations using different land covers, that is, 0.13–0.75 mm day^{-1} in any of the five circulation conditions (calculated from the rows in Table 2). These results indicate that the

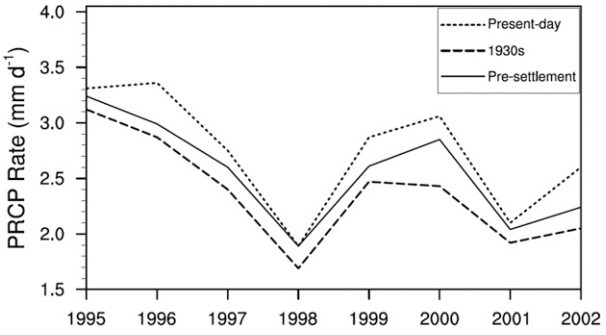

FIG. 2. Time series of simulated May–July precipitation in the U.S. Great Plains using different land cover and the same present-day circulation.

effect of land-cover change on May–July precipitation anomaly in the U.S. Great Plains has a magnitude comparable to that from the large-scale circulation forcing. When the latter is weak, the former could play a prominent role in drought development and maintenance.

This role of land-cover change on the 1930s Dust Bowl drought can also be delineated from a different perspective again using the results of our experiments in Table 2. Records of precipitation show that May–July precipitation in the U.S. Great Plains was 2.66 mm day^{-1} during 1995–2002, slightly below the 1971–2000 average of 2.71 mm day^{-1} [these precipitation values are calculated from the UK Climate Research Unit (CRU) 3.23 dataset]. In other words, the SST and atmospheric circulation variation during 1995–2002 did not cause any long-lived severe drought in the U.S. Great Plains under its existing land cover. However, when this same circulation is used in the model in conjunction with the 1930s land cover, the simulated precipitation is persistently lower than from using the present-day land cover or the presettlement land cover. This persistent land-cover effect is shown in both the mean precipitation over the simulation period (rows in Table 2) and the transient process in that period (Fig. 2). Figure 2 shows the simulated May–July precipitation using the same large-scale circulation and three different land-cover scenarios. The difference between the precipitation time series from simulations using the 1930s land cover and using the presettlement (and present day) land cover is statistically significant at the 95% confidence level from the Student's *t* test.

In addition to showing the persistently lower precipitation from using the 1930s land cover, Fig. 2 also shows large amplitude interannual precipitation variation. Its relationship with the land-cover change induced persistently lower precipitation anomaly in Fig. 2 suggests that variation is an effect of the circulation. Thus, Fig. 2 shows that the large-scale circulation still determines the general pattern of precipitation anomalies. The land-cover effect, although potentially of comparable magnitude, is to enhance and prolong the initial negative anomaly or drought that is initiated by remote forcing variability.

In the 1930s Dust Bowl drought, mild ENSO events in the tropical Pacific and the AMO SST anomaly in the North Atlantic, or the nonlinearity of the circulation (Hoerling et al. 2009), could have provided a circulation condition to initiate the drought. The drought was able to intensify and prolong for multiple years because of the particular land-cover condition and its effect to persistently suppress the precipitation. These processes are similar to those discussed by Cook et al. (2009). While Cook et al. (2009) suggest that the land-cover effect is to enhance subsidence, we propose in the following an additional effect of land cover that substantially weakens moisture fluxes into the Great Plains and undermines development of precipitation.

Our analysis of the model results shows that the drastic land-cover change from presettlement to the 1930s in the Great Plains resulted in a strong increase in the surface albedo (Fig. 3a). On average, the albedo changes from ~0.16 in the native grassland to ~0.20 in dryland cropland, and such a change can considerably alter the surface energy budget (e.g., Hartmann 1994). In our simulations, changes in surface albedo from the presettlement to the 1930s land-cover resulted in a 5 W m^{-2} reduction in solar energy absorbed at the surface (averaged over the Great Plains from May to July). Reduced absorption of solar radiation lowers the available energy at the surface. This energy reduction is shown in Fig. 3b by the large decrease in net radiation at the surface with the 1930s land cover, especially over dryland croplands/pastures and bare soils. Decrease of net radiation at the surface further causes reduction in atmospheric energy which is primarily sustained by radiation from the surface. Surface sensible heat even in high surface temperatures during a drought is a small fraction of the energy to the atmosphere (e.g., Charney 1975; Hartmann 1994). A strong decrease in atmospheric energy results in strong subsidence that keeps a stable thermodynamic profile by heating the atmosphere through adiabatic compression (Fig. 3c). In the meantime, the subsidence suppresses convection and precipitation. This direct drying effect of land cover was introduced in Charney (1975) and has been identified and suggested as working to intensify the 1930s Dust Bowl drought (Seager et al. 2005; Cook et al. 2009).

As we have previously indicated, this direct subsidence drying effect will be short-lived in the U.S. Great Plains if there is sufficient large-scale moisture supply to the region, because convection will develop along the

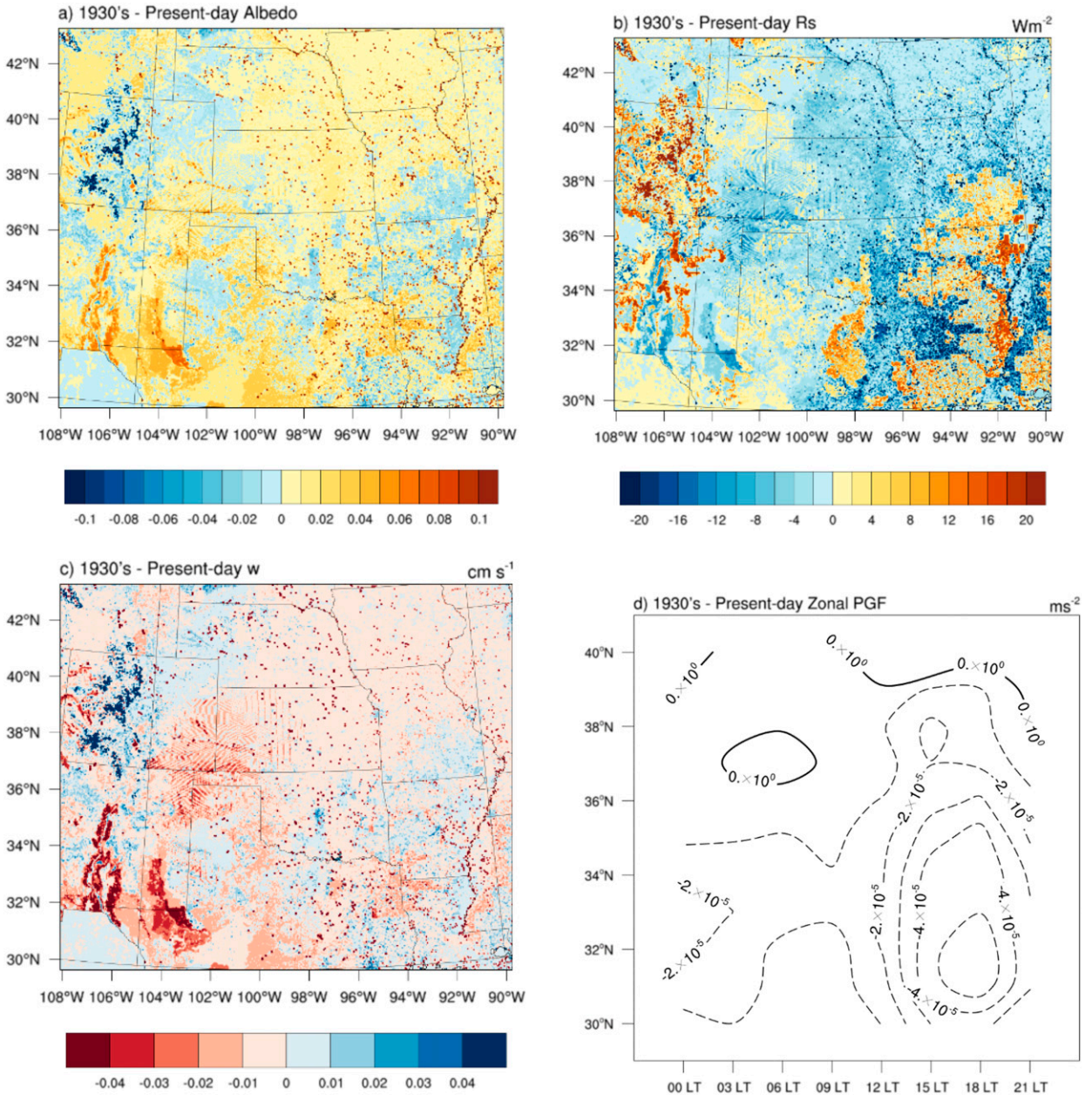

FIG. 3. Differences (values obtained from the simulation using the 1930s land-cover minus the values obtained from simulation using the present-day land cover under the same SST and large-scale circulation) of (a) surface albedo, (b) net radiation budget at the surface (Rs; W m^{-2}), (c) atmospheric vertical motion driven solely by the atmospheric energy balance (cm s^{-1}), and (d) zonal PGF (m s^{-2}) calculated between 95° and 100°W for each latitude from 30° to 40°N and averaged at local time (LT) marked on the abscissa averaged over May–July (the dashed lines are for weakened PGF). The tiny dots in (a)–(c) are water bodies that have distinctively different albedo from the land. In (b) and (c), wave patterns over Kansas, Colorado, Texas, Oklahoma, and New Mexico result from how bare soil was added to the land cover.

boundaries between the subsiding dry areas and the moist air to the south and east, such as the dryline, and bring intense convection and precipitation (Hane et al. 1997). Thus, some additional process must act to undercut the moisture supply to the region in order to amplify and sustain the drought.

That process could rise from an indirect effect of and be sustained by the 1930s land cover in the Great Plains. In the warm season, the U.S. Great Plains normally has low pressure in the lower troposphere, relative to the high pressure in the subtropical North Atlantic (Palmén and Newton 1969). Our results show that the enhanced

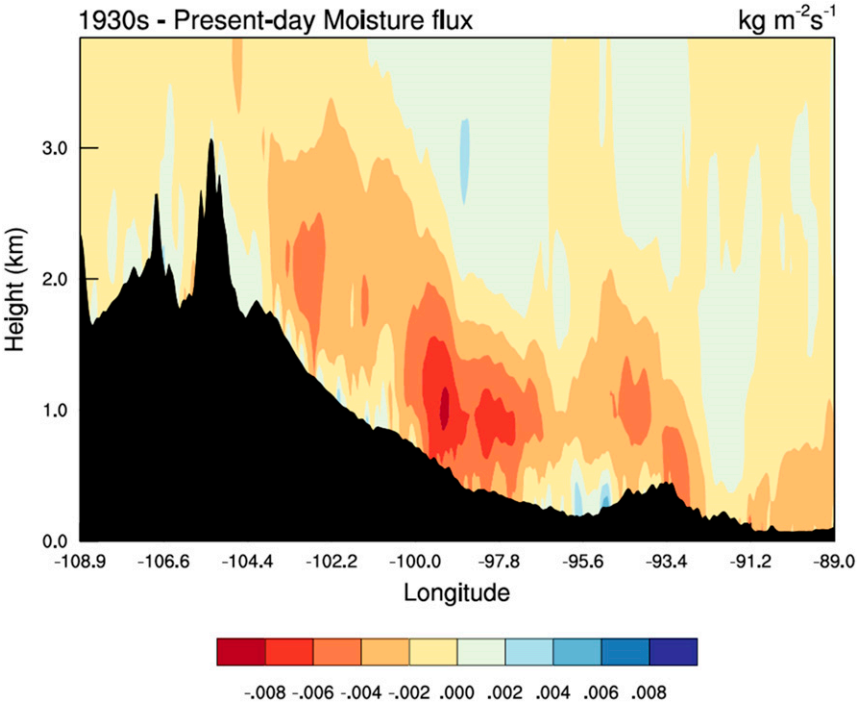

FIG. 4. Meridional water flux at the GPLLJ entrance across 36°N latitude at midnight local time ($kg\,m^{-2}\,s^{-1}$).

subsidence indicated in Fig. 3c causes a considerable increase in pressure in the lower troposphere and at the surface. Increased surface pressure in the Great Plains weakens the zonal pressure gradient force (PGF) pointing from the subtropical North Atlantic Ocean to the U.S. Great Plains. The weakened zonal PGF is shown in Fig. 3d. Because of the Coriolis effect, a weakened zonal PGF leads to a weakened GPLLJ, thereby undermining the moisture supply from the Gulf of Mexico to the U.S. Great Plains. It is intriguing to also note that in Fig. 3d the maximum weakening of the PGF happens between later afternoon hours and midnight when the GPLLJ is relatively strong (Bonner and Paegle 1970; Mo et al. 1997). Weakening of the GPLLJ, which has been observed during the 1930s Dust Bowl drought from reconstructed data (Brönnimann et al. 2009), reduces the supply of moisture to the Great Plains, as confirmed in Fig. 4. From the results in Fig. 4, our calculations show that moisture supply is reduced, relative to the present-day amount, by $3.48 \times 10^6\,kg\,m^{-1}\,h^{-1}$ in a cross section from the surface to 700 hPa along 36°N latitude between 92° and 105°W longitude. It corresponds to 0.9 $mm\,day^{-1}$ precipitation reduction in the Great Plains averaged for May–July. This reduction rate is similar to that observed during the 1930s Dust Bowl drought (cf. Figs. 5a and 5c). The same process and resulting decrease in May–July precipitation in the Great Plains are found in comparisons between simulations using the 1930s land cover and the presettlement land cover (Fig. 5b).

4. Concluding remarks

Using high-resolution modeling experiments we quantified an effect of the particular land cover in the 1930s in the U.S. Great Plains that weakens the southerly moisture flux into the region and suppresses May–July precipitation. By lowering the average precipitation, this particular land-cover effect makes the Great Plains more susceptible to drought. When drought occurs, possibly initiated by remote forcing, the land-cover effect enhances its intensity and prolongs its duration.

This land-cover effect is achieved by modifying the regional atmospheric circulation. It is tested and shown to be persistent in different circulations (e.g., the present-day circulation and circulations forced by AMO warm and cold phases). Results from those tests also suggest a static nature of this land-cover effect because it does not change the course of the precipitation variation that is described in the large-scale circulation. Therefore, while lowering the precipitation must have contributed to the Dust Bowl drought by the 1930s land-cover effect, the initiation as well as the recovery of

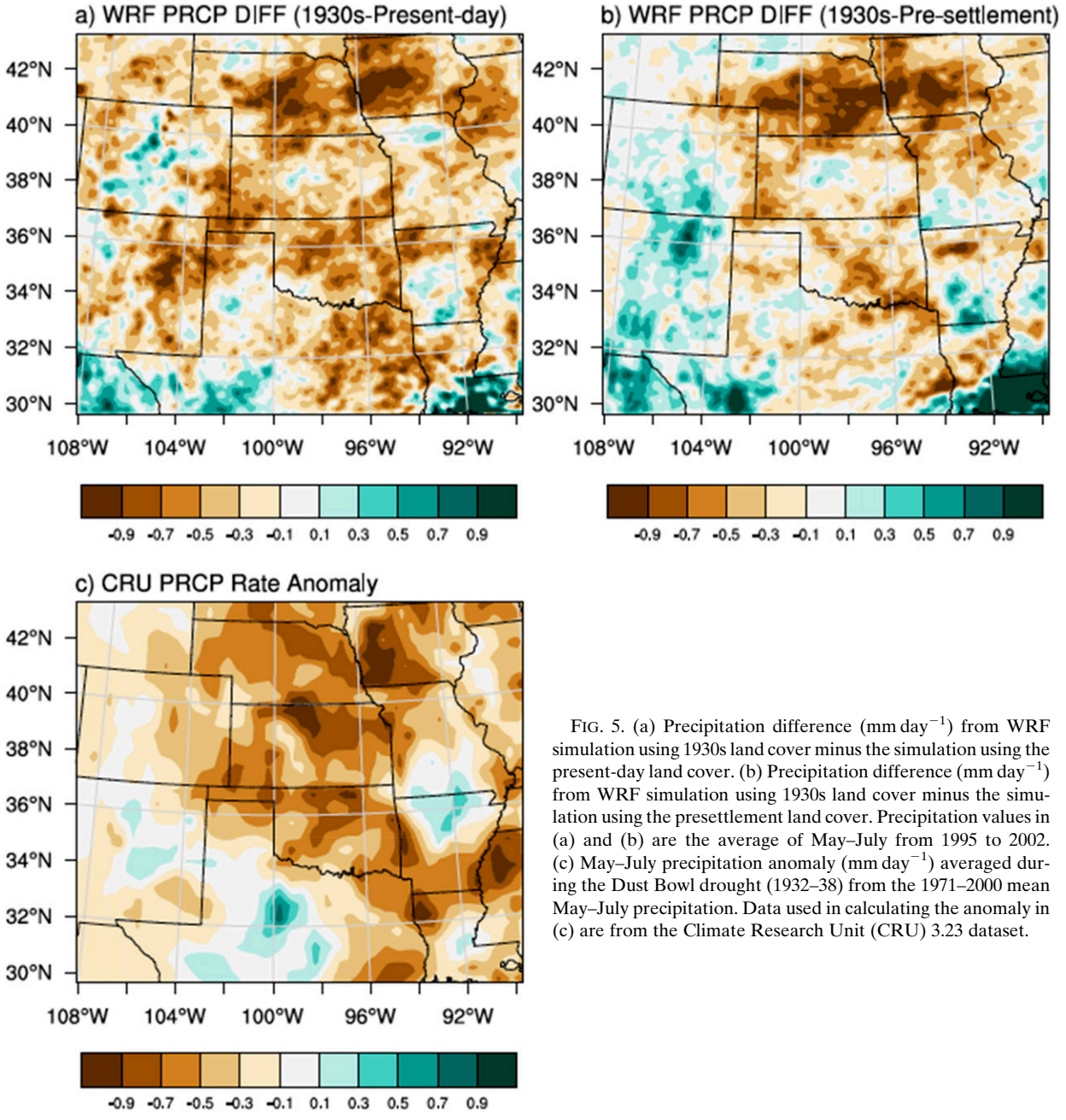

FIG. 5. (a) Precipitation difference (mm day^{-1}) from WRF simulation using 1930s land cover minus the simulation using the present-day land cover. (b) Precipitation difference (mm day^{-1}) from WRF simulation using 1930s land cover minus the simulation using the presettlement land cover. Precipitation values in (a) and (b) are the average of May–July from 1995 to 2002. (c) May–July precipitation anomaly (mm day^{-1}) averaged during the Dust Bowl drought (1932–38) from the 1971–2000 mean May–July precipitation. Data used in calculating the anomaly in (c) are from the Climate Research Unit (CRU) 3.23 dataset.

that drought would likely result from the large-scale circulation change, either of some chaotic origin (Hoerling et al. 2009) or forced by weak SST anomalies (e.g., Schubert et al. 2004), or combinations of both (e.g., McCabe et al. 2004).

From a broader perspective, our findings indicate that certain regional-scale terrestrial processes can substantially increase the vulnerability and susceptibility to severe and prolonged droughts. By reducing such vulnerability through sustainable policies and practices, humans could improve the natural system and their living environment.

Acknowledgments. We thank anonymous reviewers whose comments and suggestions helped improve this work considerably. This research has been supported by the National Science Foundation (Grant AGS-1355916). Jose Abraham Torres-Alavez was partially supported by a graduate scholarship of Mexico (CONACYT, Registry 361205). We thank Dr. Robert Oglesby and Ms. Cindy Hays

for collaborations in early stages of the modeling work and Dr. David Wedin for helpful discussions. We would like to acknowledge high-performance computing support from Yellowstone (ark:/85065/d7wd3xhc) provided by NCAR's Computational and Information Systems Laboratory, sponsored by the National Science Foundation.

REFERENCES

Bonner, W. D., and J. Paegle, 1970: Diurnal variations in boundary layer winds over the south-central United States in summer. *Mon. Wea. Rev.*, **98**, 735–744, https://doi.org/10.1175/1520-0493(1970)098<0735:DVIBLW>2.3.CO;2.

Brönnimann, S., and Coauthors, 2009: Exceptional atmospheric circulation during the "Dust Bowl." *Geophys. Res. Lett.*, **36**, L08802, https://doi.org/10.1029/2009GL037612.

Brubaker, K. L., D. Entekhabi, and P. S. Eagleson, 1993: Estimation of continental precipitation recycling. *J. Climate*, **6**, 1077–1089, https://doi.org/10.1175/1520-0442(1993)006<1077:EOCPR>2.0.CO;2.

Bukovsky, M. S., and D. J. Karoly, 2009: Precipitation simulations using WRF as a nested regional climate model. *J. Appl. Meteor. Climatol.*, **48**, 2152–2159, https://doi.org/10.1175/2009JAMC2186.1.

Charney, J. G., 1975: Dynamics of deserts and drought in the Sahel. *Quart. J. Roy. Meteor. Soc.*, **101**, 193–202, https://doi.org/10.1002/qj.49710142802.

Cook, B. I., R. L. Miller, and R. Seager, 2009: Amplification of the North American "Dust Bowl" drought through human-induced land surface degradation. *Proc. Natl. Acad. Sci. USA*, **106**, 4997–5001, https://doi.org/10.1073/pnas.0810200106.

Cunfer, G., 2005: *On the Great Plains: Agriculture and Environment*. Texas A&M, 292 pp.

Dudhia, J., 1989: Numerical study of convection observed during the Winter Monsoon Experiment using a mesoscale two-dimensional model. *J. Atmos. Sci.*, **46**, 3077–3107, https://doi.org/10.1175/1520-0469(1989)046<3077:NSOCOD>2.0.CO;2.

Enfield, D. B., A. M. Mestas-Nuñez, and P. J. Trimble, 2001: The Atlantic multidecadal oscillation and its relation to rainfall and river flows in the continental U.S. *Geophys. Res. Lett.*, **28**, 2077–2080, https://doi.org/10.1029/2000GL012745.

EPA, 2013: Level III and IV ecoregions of the continental United States. U.S. Environmental Protection Agency, accessed June 2014, https://catalog.data.gov/dataset/u-s-level-iiiand-iv-ecoregions-u-s-epa.

Gutmann, M. P., 2005: Great Plains population and environment data: Agricultural data, 1870–1997 [United States], ICPSR04254-v1. Inter-University Consortium for Political and Social Research, Ann Arbor, MI, accessed June 2014, https://doi.org/10.3886/ICPSR04254.v1.

Hane, C. E., H. B. Bluestein, T. M. Crawford, M. E. Baldwin, and R. M. Rabin, 1997: Severe thunderstorm development in relation to along-dryline variability: A case study. *Mon. Wea. Rev.*, **125**, 231–251, https://doi.org/10.1175/1520-0493(1997)125<0231:STDIRT>2.0.CO;2.

Hartmann, D. L., 1994: The energy balance of the surface. *Global Physical Climatology*, D. L. Hartmann, Ed., International Geophysics Series, Vol. 56, Academic Press, 81–114.

Higgins, R. W., K. C. Mo, and Y. Yao, 1998: Interannual variability of the U.S. summer precipitation regime with emphasis on the southwestern monsoon. *J. Climate*, **11**, 2582–2606, https://doi.org/10.1175/1520-0442(1998)011<2582:IVOTUS>2.0.CO;2.

Hoerling, M., X.-W. Quan, and J. Eischeid, 2009: Distinct causes for two principal U.S. droughts of the 20th century. *Geophys. Res. Lett.*, **36**, L19708, https://doi.org/10.1029/2009GL039860.

Homer, C. G., and Coauthors, 2015: Completion of the 2011 National Land Cover Database for the conterminous United States—Representing a decade of land cover change information. *Photogramm. Eng. Remote Sens.*, **81**, 345–354.

Hong, S.-Y., J. Dudhia, and S.-H. Chen, 2004: A revised approach to ice microphysical processes for the bulk parameterization of clouds and precipitation. *Mon. Wea. Rev.*, **132**, 103–120, https://doi.org/10.1175/1520-0493(2004)132<0103:ARATIM>2.0.CO;2.

——, Y. Noh, and J. Dudhia, 2006: A new vertical diffusion package with an explicit treatment of entrainment processes. *Mon. Wea. Rev.*, **134**, 2318–2341, https://doi.org/10.1175/MWR3199.1.

Hu, Q., and S. Feng, 2001: Variation of teleconnection of ENSO and interannual variation of summer rainfall in the central United States. *J. Climate*, **14**, 2469–2480, https://doi.org/10.1175/1520-0442(2001)014<2469:VOTOEA>2.0.CO;2.

——, and ——, 2008: Variation of the North American summer monsoon regimes and the Atlantic multidecadal oscillation. *J. Climate*, **21**, 2371–2383, https://doi.org/10.1175/2007JCLI2005.1.

——, and ——, 2012: AMO- and ENSO-driven summertime circulation and precipitation variations in North America. *J. Climate*, **25**, 6477–6495, https://doi.org/10.1175/JCLI-D-11-00520.1.

——, and M. C. Veres, 2016: Atmospheric responses to North Atlantic SST anomalies in idealized experiments. Part II: North American precipitation. *J. Climate*, **29**, 659–671, https://doi.org/10.1175/JCLI-D-14-00751.1.

——, S. Feng, and R. J. Oglesby, 2011: Variations in North American summer precipitation driven by the Atlantic multidecadal oscillation. *J. Climate*, **24**, 5555–5570, https://doi.org/10.1175/2011JCLI4060.1.

Hu, X.-M., J. W. Nielsen-Gammon, and F. Zhang, 2010: Evaluation of three planetary boundary layer schemes in the WRF Model. *J. Appl. Meteor. Climatol.*, **49**, 1831–1844, https://doi.org/10.1175/2010JAMC2432.1.

Kain, J. S., and J. M. Fritsch, 1990: A one-dimensional entraining/detraining plume model and its application in convective parameterization. *J. Atmos. Sci.*, **47**, 2784–2802, https://doi.org/10.1175/1520-0469(1990)047<2784:AODEPM>2.0.CO;2.

Lawrence, D. M., and Coauthors, 2011: Parameterization improvements and functional and structural advances in version 4 of the Community Land Model. *J. Adv. Model. Earth Syst.*, **3**, M03001, https://doi.org/10.1029/2011MS00045.

McCabe, G. J., M. A. Palecki, and J. L. Betancourt, 2004: Pacific and Atlantic Ocean influences on multidecadal drought frequency in the United States. *Proc. Natl. Acad. Sci. USA*, **101**, 4136–4141, https://doi.org/10.1073/pnas.0306738101.

Mesinger, F., and Coauthors, 2006: North American Regional Reanalysis. *Bull. Amer. Meteor. Soc.*, **87**, 343–360, https://doi.org/10.1175/BAMS-87-3-343.

Mlawer, E. J., S. J. Taubman, P. D. Brown, M. J. Iacono, and S. A. Clough, 1997: Radiative transfer for inhomogeneous atmospheres: RRTM, a validated correlated-k model for the longwave. *J. Geophys. Res.*, **102**, 16 663–16 682, https://doi.org/10.1029/97JD00237.

Mo, K. C., J. Nogues Paegle, and R. W. Higgins, 1997: Atmospheric process associated with summer floods and droughts in the central United States. *J. Climate*, **10**, 3028–3046, https://doi.org/10.1175/1520-0442(1997)010<3028:APAWSF>2.0.CO;2.

Oleson, K. W., and Coauthors, 2010: Technical description of version 4.0 of the Community Land Model (CLM). NCAR Tech. Note NCAR/TN-478+STR, 257 pp., https://doi.org/10.5065/D6FB50WZ.

Omernik, J. M., and G. E. Griffith, 2014: Ecoregions of the conterminous United States: Evolution of a hierarchical spatial framework. *Environ. Manage.*, **54**, 1249–1266, https://doi.org/10.1007/s00267-014-0364-1.

Palmén, E., and C. W. Newton, 1969: *Atmospheric Circulation Systems: Their Structure and Physical Interpretation*. International Geophysics Series, Vol. 13, Academic Press, 603 pp.

Pei, L., N. Moore, S. Zhong, L. Luo, D. W. Hyndman, W. E. Heilman, and Z. Gao, 2014: WRF Model sensitivity to land surface model and cumulus parameterization under short-term climate extremes over the southern Great Plains of the United States. *J. Climate*, **27**, 7703–7724, https://doi.org/10.1175/JCLI-D-14-00015.1.

Qiao, F., and X.-Z. Liang, 2015: Effects of cumulus parameterizations on predictions of summer flood in the central United States. *Climate Dyn.*, **45**, 727–744, https://doi.org/10.1007/s00382-014-2301-7.

Ropelewski, C. F., and M. S. Halpert, 1986: North American precipitation and temperature patterns associated with the El Niño/Southern Oscillation (ENSO). *Mon. Wea. Rev.*, **114**, 2352–2362, https://doi.org/10.1175/1520-0493(1986)114<2352:NAPATP>2.0.CO;2.

Schubert, S. D., M. J. Suarez, P. J. Pegion, R. D. Koster, and J. T. Bacmeister, 2004: On the cause of the 1930s Dust Bowl. *Science*, **303**, 1855–1859, https://doi.org/10.1126/science.1095048.

Seager, R., Y. Kushnir, C. Herweijer, N. Naik, and J. Velez, 2005: Modeling of tropical forcing of persistent droughts and pluvials over western North America: 1856–2000. *J. Climate*, **18**, 4065–4088, https://doi.org/10.1175/JCLI3522.1.

Sellers, P. J., 1985: Canopy reflectance, photosynthesis and transpiration. *Int. J. Remote Sens.*, **6**, 1335–1372, https://doi.org/10.1080/01431168508948283.

Skamarock, W. C., and Coauthors, 2008: A description of the Advanced Research WRF version 3. NCAR Tech. Note NCAR/TN-4751+STR, 113 pp., http://dx.doi.org/10.5065/D68S4MVH.

Steyaert, L. T., and R. G. Knox, 2008: Reconstructed historical land cover and biophysical parameters for studies of land–atmosphere interactions within the eastern United States. *J. Geophys. Res.*, **113**, D02101, https://doi.org/10.1029/2006JD008277.

USDA, 1954: Map 2579. Soil Conservation Service, https://www.nrcs.usda.gov/wps/portal/nrcs/detail/national/about/history/?cid=stelprdb1049437.

Van Den Broeke, M. S., A. Kalin, J. A. Torres Alavez, R. Oglesby, and Q. Hu, 2017: A warm-season comparison of WRF coupled to the CLM4.0, Noah-MP, and Bucket hydrology land surface schemes over the central USA. *Theor. Appl. Climatol.*, https://doi.org/10.1007/s00704-017-2301-8, in press.

Wolter, K., and M. S. Timlin, 2011: El Niño/Southern Oscillation behaviour since 1871 as diagnosed in an extended multivariate ENSO index (MEI.ext). *Int. J. Climatol.*, **31**, 1074–1081, https://doi.org/10.1002/joc.2336.